The optically selected AGN population at high redshift

Matthew P. Hunt
Advisor: Charles C. Steidel

7 December 2001

Abstract

AGN have long been used to study the high-redshift universe, because they are often luminous and relatively easy to identify from their colors or emission lines. However, virtually all AGN studied at high redshift are drawn from the bright end of the QSO luminosity function (LF), and little is known about medium- and low-luminosity AGN at high redshift. I propose to use existing and new survey data to study the luminosity function and spectroscopic properties of these objects, with emphasis on their contribution to the ionizing background radiation field and their relationship to Lyman break galaxy properties.

1 Background and scientific justification

In recent years, several groups have studied the QSO population at high redshift in order to measure properties such as the luminosity function and AGN fraction. Some of these studies, using the Sloan Digital Sky Survey (York, 2000; Fan *et al.*, 2001) or Second Palomar Sky Survey (Kennefick *et al.*, 1995), select QSOs on the basis of their photometric colors, while others select QSOs from their emission lines (Schmidt *et al.*, 1995). However, they all have one important deficiency in common: Their photometric and spectroscopic depth is only adequate for studying the most luminous QSOs at high redshift ($z \sim 3$).

As a result, our picture of the QSO population at high redshift is incomplete. In general, researchers use the luminosity function of the local universe as a template for the luminosity function at high redshift; most assume that the evolution is pure luminosity evolution, in which the characteristic luminosity is a function of redshift (Boyle *et al.*, 2000). Pure density evolution, in which only the normalization is a function of redshift, has been ruled out by modern surveys.

The general trend is that the QSO luminosity function predicts a small density of QSOs at the start of galaxy formation, $z \gtrsim 3$, increases to a peak around $z \sim 2$, and then decreases to the level of the local universe. Various functional forms are used for the luminosity function; a double power law is most typical, with the power-law "break" falling at $L = L_\star$. The luminosity evolution is quite strong from the local universe to at least $z \sim 2.2$, with $L_\star(z) = L_{\star,0}(1+z)^k$ and $k \approx 3.15$ providing a good fit in the optical (Boyle *et al.*, 1988) and the X-ray (Jones *et al.*, 1997). At $z \gtrsim 2.2$, a different form is necessary; a Gaussian in z peaked at $z \sim 2.75$ provides an adequate fit (Pei, 1995), but is not well constrained and arises from studies of only bright quasars.

Understanding the QSO luminosity function in detail is important, because QSOs are likely an important contributor to the UV radiation field which reionized the universe at $z \gtrsim 6$ (Djorgovski *et al.*, 2001; Becker *et al.*, 2001). While the accounting of sources is much different at $z \sim 3$, it is still interesting to determine the relative contributions of star-forming galaxies and AGN. We have already determined that a non-negligible fraction of the ionizing background comes from Lyman continuum photons leaking from star-forming

galaxies (Steidel *et al.*, 2001); measuring the contribution from QSOs will provide an accounting which is independent of other methods. Also, the reionization of He II occurs at $z \sim 3$ and requires the hard UV spectrum of AGN due to its 54.4 eV ionization potential.

Many researchers have studied the presence of central massive black holes (MBHs) in normal and active galaxies, using stellar dynamics (Ghez *et al.*, 1998; Kormendy and Richstone, 1995) in the case of the Milky Way and nearby normal galaxies, or reverberation mapping (Blandford and McKee, 1982) in the case of AGN. It is clear that the MBH mass and bulge luminosity are correlated in the cases of normal galaxies (Magorrian *et al.*, 1998), bright, low-redshift QSOs (Laor, 1998), and low-redshift Seyfert 1 AGN (Wandel, 1999). The Seyfert 1 galaxies have a substantially lower black hole to bulge mass ratio than luminous QSOs, which is consistent with the interpretation that Seyfert 1 AGN are in a sub-Eddington accretion phase, whereas QSOs come later in a period of exponential, Eddington-limited black hole growth, and hence have larger black hole masses (Wandel, 1999). In our $z \sim 3$ spectroscopic sample, we have a unique tool for studying AGN at the likely time of bulge formation. We believe the median stellar mass of Lyman break galaxies to be about $10^{10}\ h^{-2}\ M_{\odot}$ (Shapley *et al.*, 2001). Since central BHs typically have about 1% of the mass of the bulge in normal galaxies (Magorrian *et al.*, 1998) and bright QSOs (Laor, 1998), we can estimate central BH masses of about $10^{8}\ h^{-2}\ M_{\odot}$, and a corresponding Eddington luminosity of about $7 \times 10^{12}\ L_{\odot}$, or an AB magnitude of $m_{1700} \sim 20.8$. Non-AGN Lyman break galaxies near the median stellar mass have $m_{1700} \sim 24.5$. It is clear that nearly all of the AGN activity thus far observed in our sample is substantially sub-Eddington, or their black holes have not fully formed. I intend to study the relationship between the AGN and Lyman break galaxy populations at $z \sim 3$ to study in greater detail whether the AGN fraction and luminosity function are consistent with our current understanding of BH–bulge mass ratios, accretion rates, and AGN lifetimes. I will also study the evolution of the galaxy and AGN luminosity functions from $z \sim 3$ to the present in order to determine whether there is a delay between star formation and AGN activity, or whether they are coincident (as is often the case in the local universe).

There is recent evidence (Kuhn *et al.*, 2001) that luminous QSOs show no evolution in spectral index from $z = 3$ to the local universe. The result favors the model of successive generations of lower-luminosity QSOs, rather than a single population whose luminosity is decreasing. The authors also find excess flux from Fe II from 2200 Å to 3000 Å in the local sample, which is not present at high redshift. The mechanism for this increase is not at all clear; it does not seem to be related to overall Fe abundance. In this study, both the high-redshift and low-redshift samples consisted of QSOs which are luminous *compared to the characteristic luminosity at their own redshift* ($1 < L/L_{\star}(z) < 7$). Since the characteristic luminosity is much fainter in the local universe ($M_V = -22.75$ vs. $M_V = -27.5$), the study did not include high-redshift QSOs which have the same luminosity as those demonstrating the 2200–3000 Å excess. I believe that it will be instructive to compare the spectra of low-luminosity high-redshift QSOs to those of low-redshift QSOs, in order to see if features such as the Fe II bump are evident. Unfortunately, this cannot be done in the optical for $z \sim 3$ QSOs, but should be possible for $z \sim 2$ QSOs.

2 Proposed research

I propose to study the medium- and low-luminosity AGN at high redshift which have been largely omitted from the work described above. In order to make the best use of observing time, I will look for the medium-luminosity AGN separately from the low-luminosity AGN. Throughout this discussion, I will use the term "QSO" to refer to broad-line AGN without imposing a luminosity cutoff; "AGN" will refer to both broad- and narrow-line AGN.

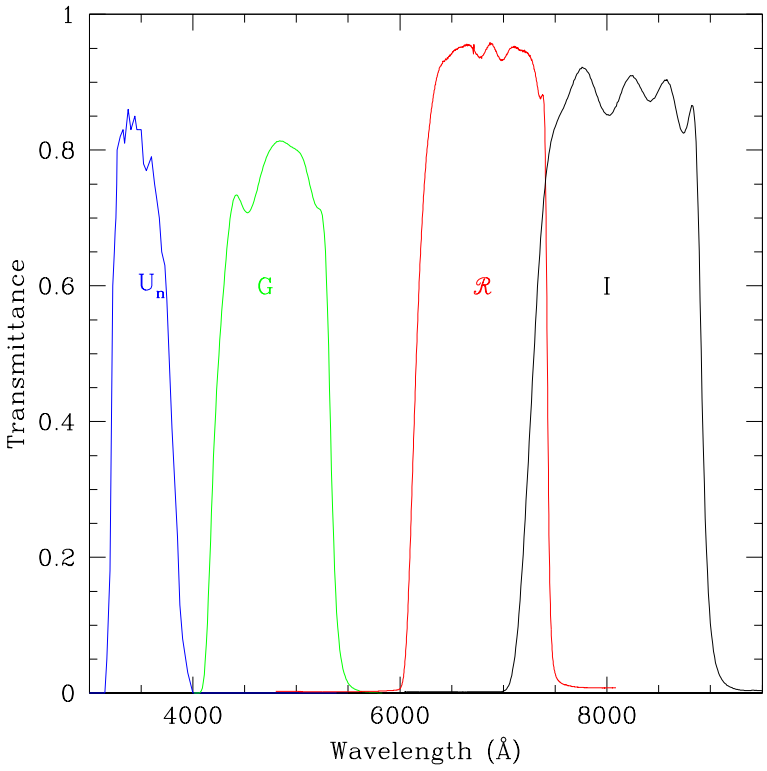

Figure 1: The U_n, G, $\mathcal{R}$, and I filter set of Steidel and Hamilton (1993).

2.1 Low-luminosity AGN

In order to study galaxies at high redshift, my advisor and collaborators have obtained a considerable amount of very deep multicolor imaging data, totaling ~ 0.6 square degrees in at least three filters, U_n (essentially identical to SDSS u'), G (essentially identical to SDSS g'), and $\mathcal{R}$, which is wider and redder than most r filters (Steidel and Hamilton, 1993; see Figure 1). Most fields also have deep imaging in our I filter (similar to SDSS z'). Magnitudes in this filter set are on the AB system (Oke and Gunn, 1983). These filters were specifically tuned to permit the selection of high-redshift galaxies based on their colors. The intrinsic spectral energy distribution (SED) of galaxies, their opacity to Lyman-continuum photons, and the opacity of the IGM produce a so-called "Lyman break" at 912 Å, with very little flux present at shorter wavelengths. The filter set is designed so that at $z \sim 3$ this break falls between U_n and G, giving a very red $U_n - G$ color despite a fairly flat $G - \mathcal{R}$ color. Similar methods can be used to select galaxies at $z \sim 4$, 2, and 1.

At high redshift, the IGM ensures that the SED of an AGN also features a Lyman break, and hence the same color selection can efficiently select AGN at the same redshifts as the target galaxies. At the photometric selection limit of our data, $\mathcal{R} \sim 25.5$, Lyman break galaxies far outnumber AGN; hence AGN are a small "contaminant" in our survey. Currently, there are 13 QSOs and 24 narrow-line AGN in our spectroscopic sample; half of the QSOs and nearly all of the narrow-line AGN are fainter than $\mathcal{R} = 23$. It is important to note that because the color signature for $z \sim 3$ selection uses the Lyman break, rather than emission lines, we are sensitive to both broad- and narrow-line AGN. I have produced composite spectra of the existing broad- and narrow-line AGN sample; see Figure 2.

Unfortunately, selecting QSOs at $z \sim 2$ is substantially more difficult, because the Lyman break falls outside the optical window. While we can efficiently select galaxies at $z \sim 2$ on the basis of the Lyman α forest, the flux decrement from the forest is offset in AGN by their

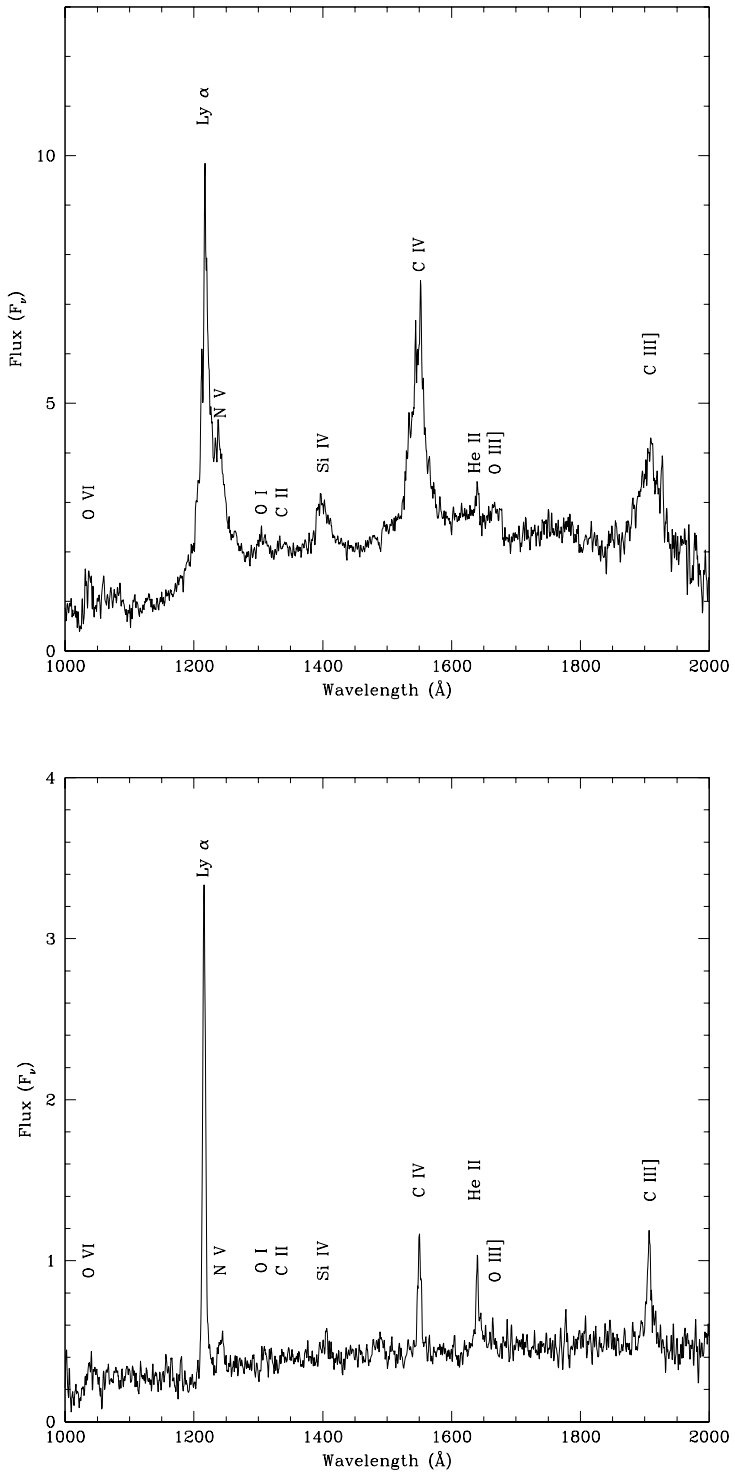

Figure 2: Composite spectra of 13 QSOs with $20.5 < \mathcal{R} < 24.8$ **(top)** and 24 narrow-line AGN ("Type II QSOs") with $22.6 < \mathcal{R} < 25.5$ **(bottom)** from our spectroscopic sample. The flux units are arbitrary. The spectra have been boxcar-smoothed by 1.6 Å.

Lyman α emission. The great variation in spectral index and emission line flux of AGN further scatters their colors, making it difficult to select them in a reasonably complete and unbiased way. The traditional method of selecting QSOs by UV excess breaks down at faint magnitudes, due to contamination from compact blue galaxies at intermediate redshift, which have similar colors. I intend to develop better methods for selecting AGN at $z \sim 2$, but realistically expect that the $z \sim 3$ sample will be more complete and better understood.

We continue to obtain deep imaging and followup spectroscopy in fields which are interesting for reasons not directly related to this thesis. Doubtless some of these photometric high-redshift galaxy candidates will turn out to be AGN and contribute to the sample of low-luminosity AGN at high redshift, improving the constraints that I can place on the luminosity and AGN fraction.

2.2 Medium-luminosity AGN

Because the deep pointings which yield faint AGN ($\mathcal{R} \sim 24$–25) require at least 10 hours of total integration time per pointing, relatively small areas of the sky can be surveyed in this fashion. Consequently, the relatively rare AGN at $\mathcal{R} \sim 21$–22 are poorly represented in our data set. Wide-field surveys generally do not go deep enough to observe these AGN (SDSS spectroscopy ends at $i' \sim 20$); hence there is a gap in luminosity between our AGN sample and those from wide-field surveys.

I propose, therefore, a shallower survey that uses the 200-inch and LFC to cover an area of about 4 square degrees. With about 1 hour of integration in each LFC pointing, it is possible to detect $z \sim 3$ AGN to $\mathcal{R} \sim 23$ using the Lyman-break method. Spectroscopic followup of candidate objects will be performed using the Double Spectrograph or LRIS as appropriate. In 4 square degrees, I expect to find about 8 QSOs with $g' < 21$, whose redshifts can be obtained in about 30 minutes each with the Double Spectrograph. I will therefore require about 40 hours of integration at Palomar. Taking into account instrument overhead and losses to weather, I seek a total of 10 nights for this project. A proposal for 6 nights was submitted for this project in semester 2002a, but the TAC has not yet announced the results. Depending on weather conditions a portion of our 5 nights in December 2001 may also be used for this project.

Koo and Kron (1988) predict about 20 QSOs per square degree with $g' < 23$ and $2.6 < z < 3.5$. Even if, as is likely the case, the estimate over-predicts the QSO density, this survey will provide an adequate sample for constraining the medium-luminosity part of the LF shape at $z \sim 3$. QSOs at lower redshift will be even more numerous, but our selection efficiency at $z \sim 2$ is not yet clear.

A side benefit of this survey, not directly part of my thesis, is that bright QSOs (whose Lyman-α forest can be measured with ESI, about $V < 22$) are useful to us as probes of the intergalactic medium. Should an LFC pointing with multiple bright QSOs be found, we can do a deep imaging followup and cross-correlate the Lyman break galaxies in the field with the IGM.

2.3 AGN at other wavelengths

Two of our deep pointings have, or will have, deep *Chandra* coverage. The Hubble Deep Field has been observed with *Chandra* ACIS for 1 Msec (Brandt *et al.*, 2001), and the Groth Westphal Survey area will be observed for 200 ksec in the summer of 2002. C. Steidel is a co-investigator on the *Chandra* GWS project, which ensures that I will have rapid access to the data. We already have extensive imaging and $z \sim 3$ spectroscopic data in these fields, including 9 AGN in the GWS and 3 in the HDF, and will obtain spectroscopy of $z \sim 2$ candidates in 2002.

A surprising result from the *Chandra* coverage of the HDF is that our spectroscopic catalog contains a galaxy with clear AGN activity, but which is undetected by *Chandra* (see Figure 3). This suggests that optical selection of AGN finds some objects which are missed

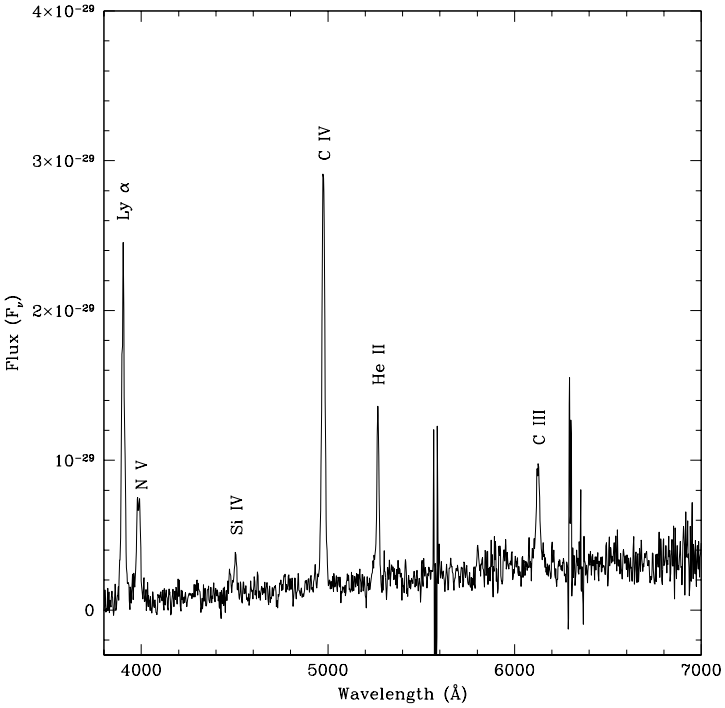

Figure 3: The galaxy HDF M49 ($z = 2.209$) which shows clear AGN activity but is undetected by *Chandra*. Strong, narrow Lyman α, N V, Si IV, He II, and C III lines emission lines are present. The C IV emission is unusually strong relative to Lyman α and He II; compare with the composite spectrum, Figure 2.

in even the deepest X-ray surveys. There is also some evidence that optically luminous QSOs at high redshift are underluminous in X-rays (Lamer *et al.*, 1997; Green *et al.*, 1995). Lamer *et al.* find that optical and ROSAT surveys which find the same number of QSOs per unit solid angle select different objects, with the optical selection favoring higher redshift QSOs, and Green *et al.* find that the optical-to-X-ray power law slope α_{ox} depends on optical luminosity, with optically luminous QSOs having a smaller L_x/L_o luminosity ratio. Using the Green *et al.* expression for α_{ox} to perform a simple calculation of the expected soft X-ray flux of a $\mathcal{R} = 24$, $z = 3$ QSO shows that it is about $F_{0.5-2.0\ \mathrm{keV}} \sim 7 \times 10^{-17}$ erg s^{-1} cm^{-2}, or just twice the sensitivity limit of the 1 Msec *Chandra* Deep Field (Brandt *et al.*, 2001). Given that α_{ox} has considerable scatter and we go deeper than $\mathcal{R} = 24$, it is not surprising that we can select some objects that are undetected in the deepest *Chandra* observations.

There has been considerable controversy relating QSO X-ray luminosity to the presence of strong optical Fe II emission. Some researchers have found that low-redshift QSOs with strong X-ray emission tend to have weak optical Fe II (Wilkes *et al.*, 1999), while the LBQS QSOs with the strongest UV Fe II emission have stronger soft X-ray fluxes than those without (Green *et al.*, 1995). Obviously, this is quite a discrepancy, and I am hopeful that our QSOs in fields with good X-ray coverage will help to resolve the issue.

3 Feasibility

3.1 Efficient selection

In order to understand the luminosity function and AGN fraction, it is important to quantify the selection function of our survey. To this end, I have been investigating the selection function for QSOs in our existing deep catalog.

One approach I have used is to convolve known QSO spectra with our filter bandpasses (along with instrumental throughput). Obviously, I cannot use the spectra of QSOs from our deep surveys, because by definition they have colors which meet our selection criteria! I have therefore used the spectra from a survey for intervening Lyman limit systems (Sargent *et al.*, 1989; Stengler-Larrea *et al.*, 1995). The QSOs used in this study were largely discovered from their emission lines in objective prism or grism surveys rather than from their colors, and hence should be selected reasonably independently from the color selection that I employ. The spectra have also been carefully flux calibrated and extend to 3200 Å, so they yield accurate colors when convolved with our filter passbands and CCD throughput model.

Our $z \sim 3$ color selection identifies 57% of the 103 QSOs included in the test (Figure 4). The QSOs are in the range of $2.7 < z < 4.1$. Selection efficiency appears slightly peaked around $z \sim 3.2$. Figure 5 shows a color-color diagram for these QSOs, along with the selection criterion. My examination of the spectra of these QSOs suggests that the ones which are not selected by our color cut have less emission line flux (relative to the continuum) than those which are selected; hence there is less flux in the G band, and the QSO misses the $U_n - G$ cut.

The SDSS QSO catalog Early Data Release (Schneider *et al.*, 2001; hereafter EDR) includes photometry and spectra of more than 3800 QSOs with spectroscopic redshifts. Our $z \sim 3$ color cuts are extremely successful in selecting the $2.8 < z < 3.5$ QSOs from the catalog (Figure 4). Our sample is more than 80% complete with respect to the EDR over this interval, and shows essentially no contamination from QSOs at redshifts far from $z \sim 3$. A color-color diagram is shown in Figure 5, with QSOs having $2.8 < z < 3.5$ specially marked. Since the EDR is not statistically complete, and it is also a color-selected sample, no concrete conclusions can be drawn from this result, but it is encouraging.

The EDR also includes a high signal-to-noise composite QSO spectrum. I intend to use this spectrum, or a similar one, as a template for Monte Carlo simulations of our selection function by varying the intervening IGM, spectral index, line strengths, and so forth, and convolving with our filter passbands.

While we have no reliable way of distinguishing AGN from Lyman break galaxies at $z \sim 3$, our experience thus far indicates that the majority of wide-field survey candidates at $\mathcal{R} < 23$ will be AGN; any normal $z \sim 3$ galaxies that are that bright will merit further study in any case.

3.2 Data reduction

Both the wide-field survey and future deep pointings will require the correct and efficient reduction of LFC imaging data. I have invested considerable time and effort on this problem, and believe that I have succeeded. I use the NOAO `mscred` IRAF package to reduce the data; the result is a photometrically calibrated, stacked, tangent-plane projection for each filter, with a World Coordinate System (WCS) in the headers to provide astrometry. On multiple occasions we have made LRIS slitmasks using this astrometry with good results. If it will allow more efficient observing, I intend to reduce the wide-field data at Palomar, so that followup observations with the Double Spectrograph can be conducted on the same observing run.

Because of the time involved in this work, and its necessity for my proposed research, I expect my LFC reduction process to constitute a chapter in my thesis. My reduction

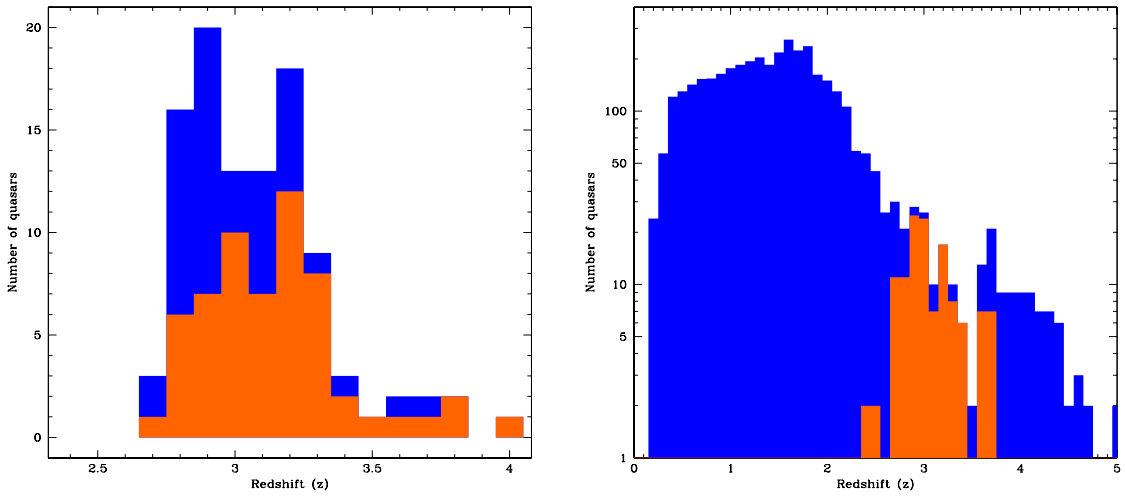

Figure 4: **Left:** The Lyman limit QSO sample is shown in blue. Objects meeting our $z \sim 3$ color selection are shown in orange. **Right:** The SDSS QSO catalog Early Data Release QSOs are shown in blue. Objects meeting our $z \sim 3$ color selection are shown in orange.

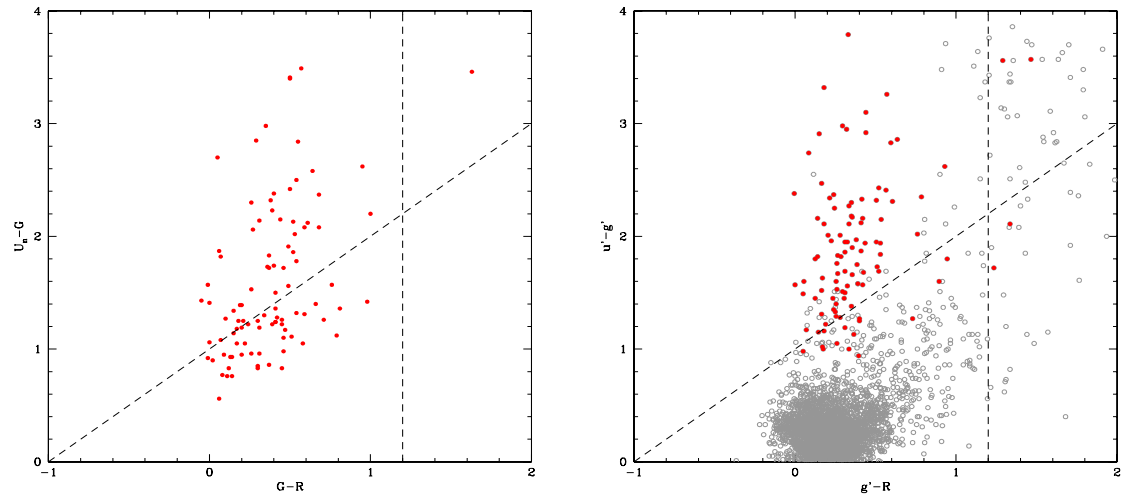

Figure 5: **Left:** Color-color diagram for the Lyman limit QSO sample. The dashed lines are the color cuts for $z \sim 3$; objects which lie above and left of the lines are selected. 8 objects with $U_n - G > 4$ are not shown but would also be selected. **Right:** Color-color diagram for the SDSS EDR, with QSOs having $2.8 < z < 3.5$ represented by filled red circles and the others by open gray circles. Our $\mathcal{R}$ filter is approximated as $(r' + i')/2$ but has little importance in the selection.

process, solutions, and software are publicly available and in use by several members of the community.

4 Timeline

- By spring 2002
  - Complete photometry for wide-field AGN survey
  - Determine whether we can efficiently select AGN at other redshifts
  - Write paper on spectra of faint AGN in existing sample
- By fall 2002
  - Investigate presence of Fe II bump in low-luminosity $z \sim 2$ sample
  - Correlate optical Fe II and other properties with *Chandra* data in HDF and GWS fields
  - Write paper with complete analysis of faint AGN in existing sample
- By spring 2003
  - Complete spectroscopy for wide-field AGN survey
- By summer 2003
  - Comment on properties of $z \sim 3$ AGN: low- vs. medium- vs. high-luminosity; high-z vs. low-z
  - Assemble complete high-redshift LF using (e.g.) SDSS and our wide and deep surveys
- By fall 2003
  - Publish complete AGN LF
  - Write up thesis

References

Becker, R. H., Fan, X., White, R. L., Strauss, M. A., Narayanan, V. K., Lupton, R. H., Gunn, J. E., Annis, J., Bahcall, N. A., Brinkmann, J., Connolly, A. J., Csabai, I., Czarapata, P. C., Doi, M., Heckman, T. M., Hennessy, G. S., Ivezic, Z., Knapp, G. R., Lamb, D. Q., McKay, T. A., Munn, J. A., Nash, T., Nichol, R., Pier, J. R., Richards, G. T., Schneider, D. P., Stoughton, C., Szalay, A. S., Thakar, A. R., and York, D. G.: 2001, *astro-ph/200108097*

Blandford, R. D. and McKee, C. F.: 1982, *ApJ* **255**, 419

Boyle, B. J., Shanks, T., Croom, S. M., Smith, R. J., Miller, L., Loaring, N., and Heymans, C.: 2000, *MNRAS* **317**, 1014

Boyle, B. J., Shanks, T., and Peterson, B. A.: 1988, *MNRAS* **235**, 935

Brandt, W. N., Alexander, D. M., Hornschemeier, A. E., Garmire, G. P., Schneider, D. P., Barger, A. J., Bauer, F. E., Broos, P. S., Cowie, L. L., Townsley, L. K., Burrows, D. N., Chartas, G., Feigelson, E. D., Griffiths, R. E., Nousek, J. A., and Sargent, W. L. W.: 2001, *astro-ph/200108404*

Djorgovski, S. G., Castro, S. M., Stern, D., and Mahabal, A.: 2001, *astro-ph/20010869*

Fan, X., Strauss, M. A., Schneider, D. P., Gunn, J. E., Lupton, R. H., Becker, R. H., Davis, M., Newman, J. A., Richards, G. T., White, R. L., Anderson, J. E., Annis, J., Bahcall, N. A., Brunner, R. J., Csabai, I. ., Hennessy, G. S., Hindsley, R. B., Fukugita, M., Kunszt, P. Z., Ivezić, Ž., Knapp, G. R., McKay, T. A., Munn, J. A., Pier, J. R., Szalay, A. S., and York, D. G.: 2001, *AJ* **121**, 54

Ghez, A. M., Klein, B. L., Morris, M., and Becklin, E. E.: 1998, *ApJ* **509**, 678

Green, P. J., Schartel, N., Anderson, S. F., Hewett, P. C., Foltz, C. B., Brinkmann, W., Fink, H., Truemper, J., and Margon, B.: 1995, *ApJ* **450**, 51
Jones, L. R., McHardy, I. M., Merrifield, M. R., Mason, K. O., Smith, P. J., Abraham, R. G., Branduardi-Raymont, G., Newsam, A. M., Dalton, G., Rowan-Robinson, M., and Luppino, G.: 1997, *MNRAS* **285**, 547
Kennefick, J. D., Djorgovski, S. G., and de Carvalho, R. R.: 1995, *AJ* **110**, 2553
Koo, D. C. and Kron, R. G.: 1988, *ApJ* **325**, 92
Kormendy, J. and Richstone, D.: 1995, *ARAA* **33**, 581
Kuhn, O., Elvis, M., Bechtold, J., and Elston, R.: 2001, *ApJ* **136**, 225S
Lamer, G., Brunner, H., and Staubert, R.: 1997, *A&A* **327**, 467
Laor, A.: 1998, *ApJ* **505**, 83L
Magorrian, J., Tremaine, S., Richstone, D., Bender, R., Bower, G., Dressler, A., Faber, S. M., Gebhardt, K., Green, R., Grillmair, C., Kormendy, J., and Lauer, T.: 1998, *AJ* **115**, 2285
Oke, J. B. and Gunn, J. E.: 1983, *ApJ* **266**, 713
Pei, Y. C.: 1995, *ApJ* **438**, 623
Sargent, W. L. W., Steidel, C. C., and Boksenberg, A.: 1989, *ApJ* **69**, 703S
Schmidt, M., Schneider, D. P., and Gunn, J. E.: 1995, *AJ* **110**, 68
Schneider, D. P., Richards, G. T., Fan, X., Hall, P. B., Strauss, M. A., Vanden Berk, D. E., Gunn, J. E., Newberg, H. J., Reichard, T. A., Stoughton, C., Voges, W., and Yanny, B. *et al.*: 2001, *astro-ph/200110629*
Shapley, A. E., Steidel, C. C., Adelberger, K. L., Dickinson, M., Giavalisco, M., and Pettini, M.: 2001, *astro-ph/200107324*
Steidel, C. C. and Hamilton, D.: 1993, *AJ* **105**, 2017
Steidel, C. C., Pettini, M., and Adelberger, K. L.: 2001, *ApJ* **546**, 665
Stengler-Larrea, E. A., Boksenberg, A., Steidel, C. C., Sargent, W. L. W., Bahcall, J. N., Bergeron, J., Hartig, G. F., Jannuzi, B. T., Kirhakos, S., Savage, B. D., Schneider, D. P., Turnshek, D. A., and Weymann, R. J.: 1995, *ApJ* **444**, 64
Wandel, A.: 1999, *ApJ* **519**, 39L
Wilkes, B. J., Kuraszkiewicz, J., Green, P. J., Mathur, S., and McDowell, J. C.: 1999, *ApJ* **513**, 76
York, D. G. *et al.*: 2000, *AJ* **120**, 1579